

NO-A176 881

COMPUTER MODELS OF THE SPACECRAFT WAKE(U) AIR FORCE  
GEOPHYSICS LAB WANSCOM AFB MA M WEINEMANN ET AL.  
24 JUL 86 AFGL-TR-86-0160

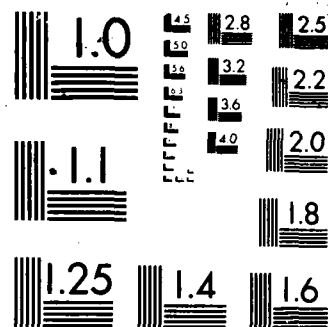
1/1

UNCLASSIFIED

F/G 20/9

NL





12

AD-A176 881

AFGL-TR-86-0160  
ENVIRONMENTAL RESEARCH PAPERS, NO. 959

## Computer Models of the Spacecraft Wake

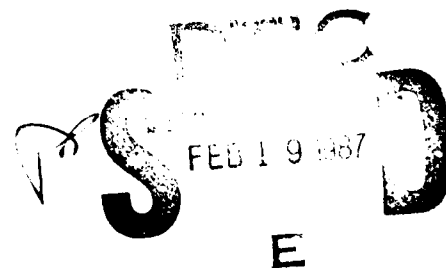
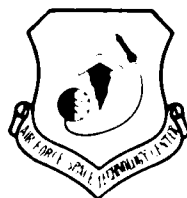
M. HEINEMANN  
A. RUBIN  
M. TAUTZ  
D. COOKE



24 July 1986



Approved for public release; distribution unlimited.



DTIC FILE COPY



SPACE PHYSICS DIVISION

PROJECT 7601

**AIR FORCE GEOPHYSICS LABORATORY**

HANSCOM AFB, MA 01731

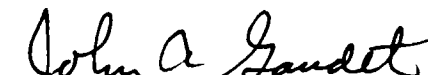
87 2 19 058

"This technical report has been reviewed and is approved for publication"

FOR THE COMMANDER



CHARLES P. PIKE, Chief  
Spacecraft Interactions Branch  
Space Physics Division



JOHN A. GAUDET, Major, USAF  
Deputy Director  
Space Physics Division

This document has been reviewed by the ESD Public Affairs Office (PA) and is releasable to the National Technical Information Service (NTIS).

Qualified requestors may obtain additional copies from the Defense Technical Information Center. All others should apply to the National Technical Information Service.

If your address has changed, or if you wish to be removed from the mailing list, or if the addressee is no longer employed by your organization, please notify AFGL/DAA, Hanscom AFB, MA 01731. This will assist us in maintaining a current mailing list.

Unclassified

SECURITY CLASSIFICATION OF THIS PAGE

REPORT DOCUMENTATION PAGE			
1a REPORT SECURITY CLASSIFICATION Unclassified		1b RESTRICTIVE MARKINGS	
2a SECURITY CLASSIFICATION AUTHORITY		3 DISTRIBUTION / AVAILABILITY OF REPORT  Approved for public release; distribution unlimited	
2b DECLASSIFICATION / DOWNGRADING SCHEDULE			
4 PERFORMING ORGANIZATION REPORT NUMBER(S) AFGL-TR-86-0160 ERP, No. 959		5 MONITORING ORGANIZATION REPORT NUMBER(S)	
6a NAME OF PERFORMING ORGANIZATION Air Force Geophysics Laboratory	6b OFFICE SYMBOL (if applicable) PHK	7a NAME OF MONITORING ORGANIZATION Air Force Geophysics Laboratory	
6c ADDRESS (City, State, and ZIP Code) Hanscom AFB Massachusetts 01731		7b ADDRESS (City, State, and ZIP Code) Hanscom AFB Massachusetts 01731	
8a NAME OF FUNDING / SPONSORING ORGANIZATION	8b OFFICE SYMBOL (if applicable)	9 PROCUREMENT INSTRUMENT IDENTIFICATION NUMBER	
8c ADDRESS (City, State, and ZIP Code)		10 SOURCE OF FUNDING NUMBERS	
		PROGRAM ELEMENT NO 62101F	PROJECT NO 7601
		TASK NO 30	WORK UNIT ACCESSION NO 01
11 TITLE (Include Security Classification) Computer Models of the Spacecraft Wake			
12 PERSONAL AUTHOR(S) M. Heinemann, A. Rubin, M. Tautz, and D. Cooke			
13a TYPE OF REPORT Scientific, Interim.	13b TIME COVERED FROM TO	14 DATE OF REPORT (Year, Month, Day) 1986 July 24	15 PAGE COUNT 30
16 SUPPLEMENTARY NOTATION Radex Corporation, Carlisle, MA			
17 COSATI CODES		18 SUBJECT TERMS (Continue on reverse if necessary and identify by block number)	
FIELD	GROUP	SUB-GROUP	
19 ABSTRACT (Continue on reverse if necessary and identify by block number) Calculations of the spacecraft interaction with the low earth orbit space plasma environment are presented, based on two computer codes, MACH and POLAR. MACH is an inside-out particle tracking code which treats spacecraft in a cylindrically symmetric grid, while POLAR is fully three dimensional. The methodology of MACH is more fundamental than that of POLAR, and MACH is used for validating the physics of POLAR in regimes where there are no comprehensive theoretical or experimental results. POLAR and MACH solutions for the wake of a charged disk in MACH 4, 5, and 8 flow are compared.			
20 DISTRIBUTION / AVAILABILITY OF ABSTRACT <input type="checkbox"/> UNCLASSIFIED / UNLIMITED <input checked="" type="checkbox"/> SAME AS RPT <input type="checkbox"/> OTIC USERS		21 ABSTRACT SECURITY CLASSIFICATION Unclassified	
22a NAME OF RESPONSIBLE INDIVIDUAL Allen Rubin		22b TELEPHONE (Include Area Code) (617) 377-2933	22c OFFICE SYMBOL PHK

DD FORM 1473, 84 MAR

83 APR edition may be used until exhausted  
All other editions are obsoleteSECURITY CLASSIFICATION OF THIS PAGE  
Unclassified

Accession For	
NTIS GRA&I	<input checked="" type="checkbox"/>
DTIC TAB	<input type="checkbox"/>
Unannounced	<input type="checkbox"/>
Justification	
By _____	
Distribution/	
Availability Codes	
Dist _____	
<b>A-1</b>	



## Summary

Until recently, computations of space plasma flow over a spacecraft have been unstable for ratios of spacecraft dimension to Debye length typical of the low earth orbit environment. We present calculations of the spacecraft/environment interaction based on two computer codes, MACH and POLAR.

We have developed MACH, an inside-out particle tracking code, for the purpose of validating the physics of POLAR in regimes where there are no comprehensive theoretical or experimental results. While the spacecraft which can be treated by MACH are restricted to simple geometries, the methodology is more fundamental than POLAR. MACH generates self-consistent solutions within the context of quasisteady Vlasov plasma flow and achieves Debye ratios previously unobtainable.

POLAR uses a three-dimensional finite-element representation of the vehicle in a staggered mesh. The plasma sheath is modeled by outside-in particle tracking. Solutions for the plasma flow, wake and vehicle charging are obtained by Vlasov-Poisson iteration; charge stabilization techniques make the results virtually insensitive to the Debye ratio. POLAR reproduces the Laframboise static plasma solutions for spherical probes and fits the Makita-Kuriki probe data for spheres in a flowing plasma in regions where comparisons are valid.

POLAR and MACH solutions for the particle and electrostatic potential structure of the wake of a charged disk in a low-altitude flow are shown for Mach numbers 4, 5, and 8. We compare the results of the codes to each other and to simple analytic approximations as part of an effort to compute the nature of the spacecraft wake and to establish the validity of the codes.

## Contents

1. INTRODUCTION	1
2. THE WAKE MODEL	4
3. COMPARISON OF MACH WITH SIMPLE ANALYTIC MODELS	9
4. COMPARISON OF MACH AND POLAR	16
5. DISCUSSION	17
REFERENCES	23

## Illustrations

1. POLAR Disk Model	6
2a. Geometrical Shadowing by a Disk at Mach 8	7
2b. Phenomenological Interaction and Wake Model for High Voltage Charging at Mach 5	7
2c. Phenomenological Interaction and Wake Model for High Voltage Charging at Mach 5 in Which the Geometric Shadowing is by the Sheath	8
3. Qualitative Model of the Ion Density Profile Along the Ram/wake Axis	8
4a. POLAR Contour Plot of the Electrostatic Potential	10
4b. POLAR Ion Trajectories	10
4c. MACH Potential Contours	11
4d. MACH Electron Density Contours	11

## Illustrations

5.	Comparison of MACH Potential and Ion Number Densities in Ram for Mach 4 and 8 With One Dimensional Sheath Contours	12
6.	Comparison of MACH Potential and Ion Number Densities Along the Rim Direction With Cylindrical Sheath Contours	14
7.	Comparison of MACH Ion Number Density Along Wake Axis With Quasineutral Wake Model Representing Geometric Shadowing for Mach 4 and 8	15
8a.	POLAR and MACH Profiles of Electrostatic Potential in Ram for Mach 5	18
8b.	POLAR and MACH Profiles of Ion Number Density in Ram for Mach 5	19
9a.	POLAR and MACH Profiles of Electrostatic Potential in the Rim Direction for Mach 5	20
9b.	POLAR and MACH Profiles of Ion Number Density in the Rim Direction for Mach 5	21
10.	POLAR and MACH Profiles of Ion Number Density in Wake	22

## Tables

1.	Typical Values of Environmental Parameters as Functions of Altitude	5
----	---	---



## Computer Models of the Spacecraft Wake

### 1. INTRODUCTION

Engineering design of spacecraft requires that computer codes, such as POLAR, be developed to simulate the spacecraft/environment interaction. In order to test such codes, there are three general lines of attack available: comparison with (1) experiment, (2) analytical results, and (3) other computer codes. These approaches are limited by the fact that comprehensive experimental results are not yet available and that the interaction between a spacecraft and a flowing plasma is sufficiently complex that no comprehensive exact solutions exist for conditions typical of the low Earth orbit environment. As a consequence, the most effective tool for code verification is comparison with other computer codes. As part of the effort involved in the development and verification of the POLAR code, we have developed an independent computer code, called MACH, designed to validate the physical and numerical methods of POLAR. MACH is constructed essentially from first principles, and can be used to examine the fundamental plasma processes in the spacecraft interaction and the formation of the wake. The purpose of this report is to discuss the results of the MACH and POLAR computer models of the spacecraft/environment interaction and wake.

---

(Received for publication 23 July 1976)

The methodologies of POLAR and MACH are somewhat different. It is these differences that make possible the validation of one code by another. POLAR (Potential of Large Spacecraft in the Auroral Regions) is designed as an engineering tool to compute the plasma interaction of large electrically complicated spacecraft in low Earth orbit. The essential differences between POLAR and its predecessor, NASCAP (which was designed for the geosynchronous environment), are that the effects of short Debye lengths, energetic auroral electrons, and the geomagnetic field, along with the formation of a supersonic ion wake, are taken into account. An essential constraint on POLAR is that the physical and numerical algorithms used must allow computations to be completed in a reasonable length of time, for example, on the order of hours or less per solution. To meet this condition, a number of novel, but essentially untested, physical assumptions have been incorporated into the code. As a consequence, the results are to be regarded as a working model whose validity is to be tested. On the other hand, POLAR is capable of accounting for the full complexity of the three-dimensional interaction within the context of the assumptions made.

The methodology of MACH (Mesothermal Auroral Charging) is somewhat closer to first principles than POLAR. MACH solves the same Vlasov-Poisson equations as POLAR but under different conditions. The most important difference is that no assumption about the sheath edge is made: the sheath and the wake are determined as the self-consistent solution to the Vlasov-Poisson equations. However, the geometry of MACH is restricted to two dimensions, precluding detailed application to real spacecraft. In addition, MACH is restricted to a single Maxwellian plasma and fixed surface potentials (that is, the surface potentials are given and not determined as a solution to a boundary value problem). MACH pays a steep price for its adherence to fundamentals: it is much less robust, requires a great deal of operator attention and requires about an order of magnitude more execution time. The MACH program is an adaptation of TDWAKE (Parker<sup>1</sup>).

In describing and comparing the two codes, we look first at the Poisson solvers. MACH uses a first order successive over-relaxation method, while POLAR uses a more sophisticated second order finite element scheme with a conjugate gradient solver. Both codes have passed a variety of Laplacian (zero plasma density) and nonflowing Poisson (nonzero plasma density) tests. These tests include the Laframboise static plasma solutions for spherical probes and the Makita-Kuriki probe data for spheres in a flowing plasma in regions where comparisons are valid. Thus, we currently dismiss Poisson solver differences as a source of discrepancy in these comparisons.

---

1. Parker, L. W. (1976) NASA Contractor Report No. CR-144159.

At this stage, we narrow our study to three possible sources of discrepancy: (1) the Vlasov solution for the number density, (2) the methods of stabilizing the Poisson solvers, and (3) grid resolution effects. The first is the greatest physical interest, the second is of numerical origin, while the third is not fundamental but must be dealt with.

The two codes differ the most in their Vlasov solutions. The inside-out method used in MACH is a standard method used in spacecraft charging models. At each grid point in the problem, each trajectory is traced backwards in time to discover whence the particle came, from the object or the ambient plasma. Use of Liouville's theorem allows the construction of the distribution function at the point and the particle number densities from the first moment of the distribution function. The method solves the Vlasov equation exactly subject only to numerical approximations, but demands an enormous number of trajectories, which are subject to cumulative numerical errors, and consequently a large amount of computation time. This method is at present too expensive for a three-dimensional code placing a priority on efficiency. Thus POLAR uses an approximate method that is efficient and whose accuracy is the focal point of this comparison. For brevity, let us assume a convergent sequence of Vlasov-Poisson iterations. Following a Poisson iteration, the solution is inspected for a sheath edge (nominally defined by electrostatic potential = 0.49 kT/e) and outside-in particle tracking is used to calculate the attracted specie number density within the sheath by weighting by the time each particle spends in each volume element. Outside the sheath, densities of attracted particles are calculated from the geometric shadow of the object. Both MACH and POLAR assume Boltzmann electrons, valid provided that the electron Mach number is small, that the surface potential is sufficiently negative that electrons do not reach the spacecraft, and that no potential wells develop. Both programs take  $\Phi = 0$  (where  $\Phi$  is the electrostatic potential) as the boundary condition at the outer grid boundary and start from an initial density distribution appropriate for the flow of a collisionless neutral gas past the spacecraft. Successive Vlasov-Poisson iteration cycles are computed until a converged solution is achieved.

The Vlasov-Poisson iteration process is inherently unstable when the Debye length is less than the grid spacing (Parker and Sullivan<sup>2</sup>). To date, only two techniques exist for treating this instability: Picard iterative mixing (Parker and Sullivan<sup>2</sup>) and charge stabilization (Cooke et al<sup>3</sup>). The latter, which is used in

2. Parker, L.W., and Sullivan, E.C. (1974) NASA Report No. TN-D-7409.

3. Cooke, D.L., Katz, I., Mandell, M.J., Lilley, J.R., Jr., and Rubin, A.G. (1985) A Three-dimensional Calculation of Shuttle Charging in Polar Orbit, Spacecraft Environmental Interactions Technology-1983, NASA CP-2359, AFGL-TR-85-0018, p. 229.

POLAR, is a correction applied at each iteration; it involves a charge density adjustment whenever it appears to be numerically amplified by finite grid resolution. The iterative mixing method presumably has less impact on the physics, but this has not been conclusively demonstrated. This accuracy issue is addressed by using both methods in MACH.

An efficient three-dimensional code must keep execution time within reasonable bounds. In order to attain this goal, POLAR is typically run with minimum spatial resolution, so that the effects of the finite grid size is a practical concern and must be dealt with in order to develop a working model.

Our ultimate aim is to develop POLAR to calculate the spacecraft interaction in a quite general way. The approach which we will present here is a bootstrap method: begin with a restricted code (MACH) which does the fundamental physics correctly, check it by available analytical and physical means, and then use it as the standard of comparison for the more general code (POLAR). In this report we present results from MACH, possibly the first code to result in a satisfactory wake and interaction model, compare them with analytical results where applicable, and discuss the POLAR code in comparison with MACH. Our conclusion will be that MACH and POLAR represent generally accurate qualitative and quantitative models of the spacecraft interaction and wake. Features of the solution which are not yet understood are discussed.

A word about the nature of the presentation is appropriate. During the preparation of the report, the computer system which runs both models failed. As a result, the discussion is based on two sets of computations: MACH at Mach 4 and 8, on the one hand, and POLAR and MACH at Mach 5 on the other; the choice of Mach numbers depends on the results in existence at the time of the failure. While the report could have been based on Mach 5 alone, the Mach number dependence was deemed important to illustrate.

## 2. THE WAKE MODEL

To compute models of the spacecraft interaction, we have specialized the spacecraft in both MACH and POLAR to charged disks in flowing plasmas. Such a problem in an unmagnetized plasma can be described in terms of three dimensionless parameters (assuming that the relative orientation of the bulk velocity and the disk normal is fixed):

$$\chi = -e\Phi/kT \quad (1)$$

$$\rho = a/\lambda_D \quad (2)$$

$$M = V/\sqrt{2kT/m_i} \quad (3)$$

Here,  $e$  is magnitude of the electron charge,  $k$  is Boltzmann's constant,  $T$  is the temperature of the ambient plasma (assumed to be the same for electrons and ions),  $a$  is the disc radius,  $\lambda_D$  (here defined as the ratio of thermal speed to plasma frequency) is the ambient ion Debye length,  $M = M_i$  is the ambient Mach number,  $V$  is the ambient bulk velocity, and  $m_i$  is the ion mass; the ions are assumed to be singly ionized. In a magnetized plasma, the ion gyroradius and magnetic field orientation would provide two additional parameters. Typical values of  $M$ ,  $kT$ , and  $\lambda_D$  typical of the low Earth orbit environment are shown as functions of altitude in Table 1. Values of the ambient electron Mach number  $M_e$  are also shown.

Table 1. Typical Values of Environmental Parameters as Functions of Altitude.  $h$  is altitude in kilometers,  $M_e$  is the ambient electron Mach number,  $M_i$  is the ambient ion Mach number,  $kT$  is the temperature in electron Volts, and  $\lambda_D$  is the Debye length in centimeters

$h$ (km)	$M_e$	$M_i$	$kT$ (eV)	$\lambda_D$ (cm)
100	0.1	20	0.02	1.0
300	0.06	10	0.036	0.1 - 0.7
500	0.03	3	0.155	0.3 - 0.6
1000	0.02	4	0.253	1.0

The disk model used in the calculations is shown in Figure 1. Note that it is not circular, but octagonal and designed to fit on a square mesh. We have chosen the following sets of the dimensionless parameters: (1)  $\chi = 1000$ ,  $\rho = 100$ , and  $M = 4$  and 8 and (2)  $\chi = 200$ ,  $\rho = 50$ , and  $M = 5$  (see Section 1). The values of  $\chi$  is consistent with moderate charging, on the order of 20 to 100 V. Typical values of  $\lambda_D$  in low Earth orbit are on the order of centimeters, so that the disc radius implied by Eq. (2) is on the order of meters. Mach 4 and 8 are somewhat less than typical of low Earth orbit satellites (on the order of Mach 10). Below, we discuss the physical features associated with the numerical results.

The qualitative features of the numerical results can be understood based on a naive discussion of the interaction. The cases presented here are for high voltage negative charging, typical of charging during ion beam operations. As a result of the high voltage, which is large in comparison with the energies of the ambient ions and electrons, the interaction near the disk is qualitatively similar to that of a high voltage probe in a static plasma: while the ambient ions stream from ram, they

are accelerated toward the disk from all directions with ions impacting the disk from both ram and wake. The ram potentials and number densities are close to those expected in a static plasma, with suitable modifications due to the ram motion of the ions: a sheath is formed and the potential follows a well understood profile (see following paragraphs). The number density decreases monotonically from the sheath to the disk in the manner required to conserve mass. Because of the wrapping of the ions around the disk, this relatively high density (on the order of but less than ambient) region exterior to the low density region surrounds the disk in both ram and wake.

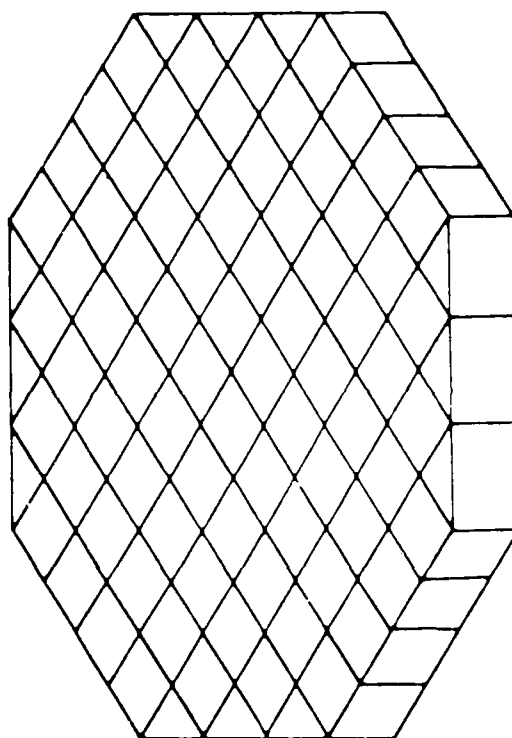


Figure 4. 190 Volt Disk Model

The far wake is quantitatively similar to simple ion and electron wrapping of the ambient plasma by the disk, which is shown for Model 1 in Figure 2. In Figure 2b we have plotted the sum of a phenomenological beam wake model and the neutral far

wake model of Alpert et al<sup>4</sup> also for Mach 8. This figure is not at all fundamental and has the status of a cartoon. The effect of the geometric shadowing is to shield the ambient plasma behind the disk, with the density being heavily depleted near the disk and approaching ambient in the far wake. Combined with the densities in the near wake, the density profile is expected to behave qualitatively as shown in Figure 3; a depletion required by mass conservation near the disk, a peak or knee near one (ram) sheath thickness in wake, a deep depletion due to geometric shadowing outside the near wake region, and gradual approach to ambient density in the far wake. Figure 2c shows the effect of increasing the shadowing radius to the sheath radius, a concept to be discussed in more detail in the following paragraphs.

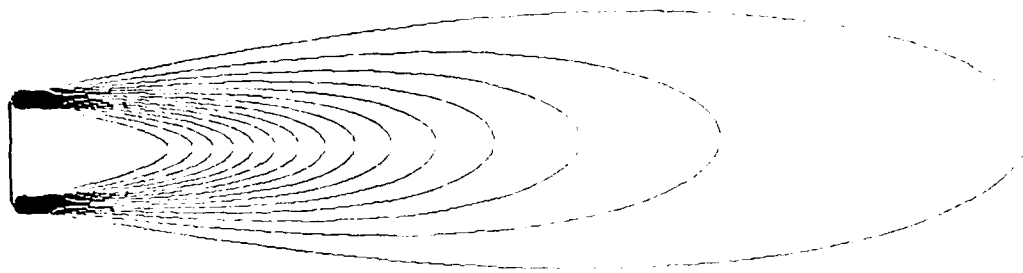


Figure 2a. Geometrical Shadowing by a Disk at Mach 8

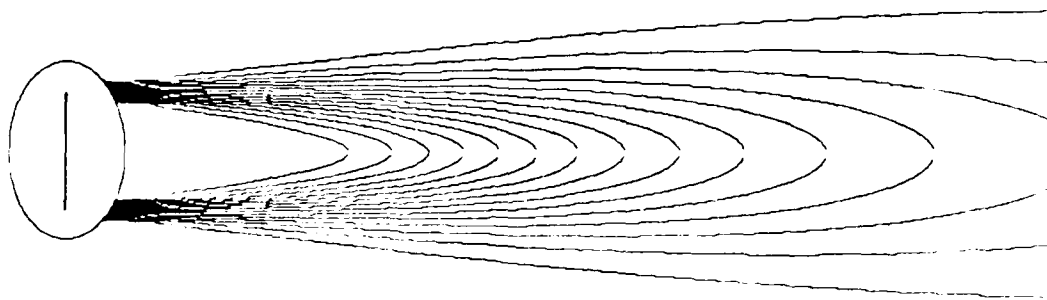


Figure 2b. Phenomenological Interaction and Wake Model for High Voltage Cathode at Mach 5. The near wake is a one-dimensional model distorted to wrap around the disk. The wake model is geometric shadowing by the disk. The contours represent ion number density; the levels are separated by one-sixteenth of the ambient density.

4. Alpert, Ya. L., Gurevich, A. V., and Pitnevskii, I. P., 1965 Space Physics With Artificial Satellites, Consultants Bureau, New York.

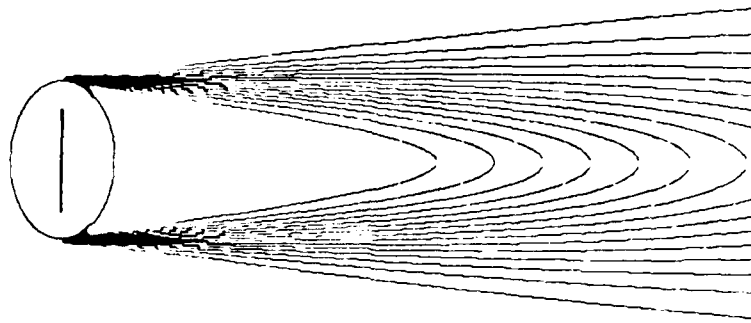


Figure 2c. Phenomenological Interaction and Wake Model for High Voltage Charging at Mach 5 in Which the Geometric Shadowing is by the Sheath

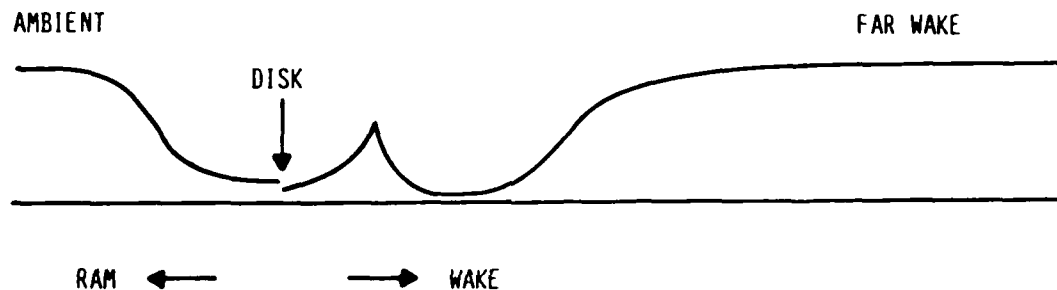


Figure 3. Qualitative Model of the Ion Density Profile Along the Ram/wake Axis

The foregoing discussion leads to the conclusion that peaks in the ion density are likely to appear in the wake, a feature which is apparent in the solutions given in the following paragraphs. A simple argument indicates that, if they occur at all, such peaks are more likely for high potentials and large Mach numbers than otherwise. The effect of the high potential is to accelerate the ion distribution function: with increasing velocity the ion distribution function narrows rapidly (Gurevich and Meshcherkin<sup>5</sup>). The acceleration of the ramming ions into the wake can thus be expected to lead to narrow ion structures on the order of a sheath thickness in wake. Low potentials and low incident Mach numbers have the effect of broadening these structures and for sufficiently low potentials and Mach numbers they certainly will not occur.

5. Gurevich, A. V., and Meshcherkin, A. P. (1981) Ion acceleration in an expanding plasma, *Sov. Phys. JETP*, 53(No. 5):937.



For purposes of comparison, we show in Figure 4a a POLAR contour plot of the electrostatic potential. This figure clearly shows the division of the potential structure into near wake and far wake. To a first approximation, the near wake is symmetric in ram and wake, much like the potential about a disk in a non-flowing plasma. The far wake is a quasineutral wake similar to the geometric shadowing of the downstream flow by the disk. The size of the near wake in comparison with the far wake is an artifact of the POLAR code. The shadowing of the ions in POLAR is due to the spacecraft only and not the spacecraft plus sheath; this problem is being corrected. Intuitively, one would expect that the narrowest part of the far wake to be about as wide as the near wake. Figure 4b shows ion trajectories from POLAR; it illustrates the nature of the ion flow on both sides of the disk, as discussed above.

Potential contours from MACH are shown in Figure 4c. In contrast to the POLAR results, the shadowing in the wake is determined by the sheath radius rather than the disk radius. The line labeled "T" is the potential  $\chi = 1$ ; the remaining contours represent  $\chi = 0.25, 0.5, \dots, 64, 128$ . The ion trajectories, which determine the charge density, have been computed for potentials above  $\chi = 0.25$ ; at lower potentials, a geometrical shadowing model has been used. The calculation was run at rather low spatial resolution, as is evident from the lengths of the straight line segments used to represent the contours. The accuracy of the contours in the far wake is not known at the present time; it is possible that they will smooth out with further relaxation of the solution. The fact that the edges of the far wake as determined by the  $\chi = 0.25$  contour are parallel is an artifact of the method: the boundaries of the computational mesh prevented it from expanding further. Electron number density contours are shown for the same solution in Figure 4d.

### 3. COMPARISON OF MACH WITH SIMPLE ANALYTICAL MODELS

The purpose of this section is to compare MACH with simple analytical models. The models used in ram and wake are reasonably good, while the model used along the edge of the disk is entirely qualitative. The purpose in these comparisons is to establish a reasonable, if inexact, basis for judging the accuracy of the models. The physical mechanisms involved in the spacecraft interaction are somewhat more complicated than the simple models. The extent of the agreement outlined in the following pages suggests that the models perform reasonably well.

POLAR WAKE MODEL

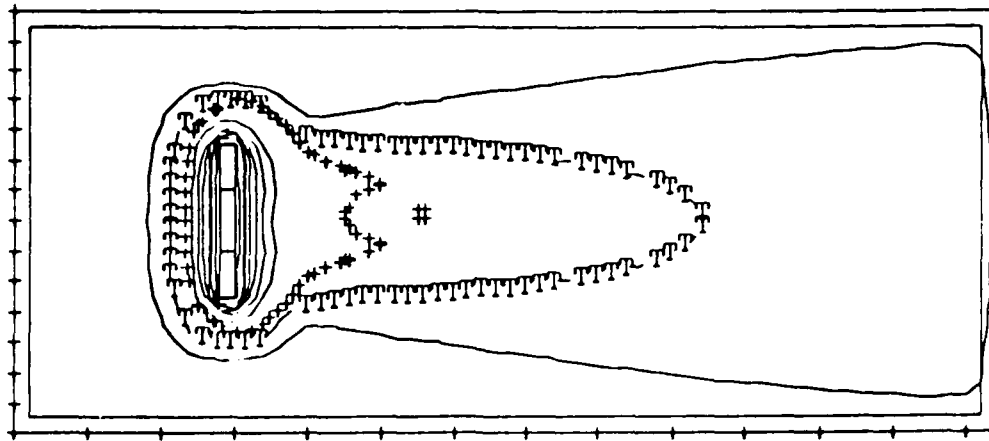


Figure 4a. POLAR Contour Plot of the Electrostatic Potential

POLAR WAKE MODEL

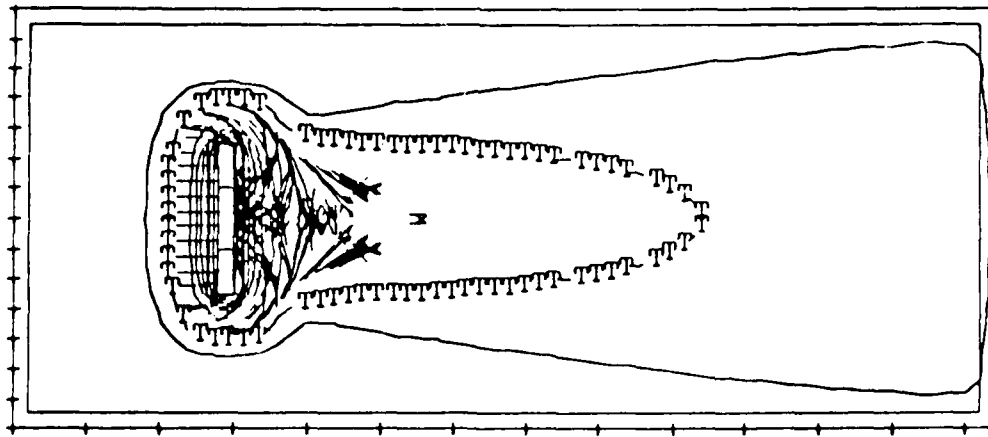


Figure 4b. POLAR Ion Trajectories

#### MACH: POTENTIAL CONTOURS

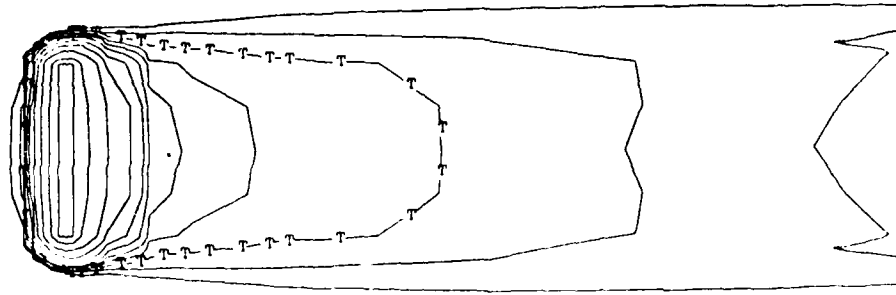


Figure 4c. MACH Potential Contours

#### MACH: ELECTRON DENSITY CONTOURS

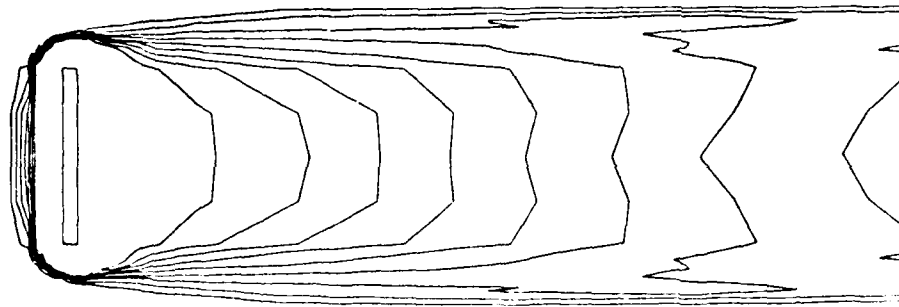


Figure 4d. MACH Electron Density Contours

Figure 5 shows the comparison of MACH potential and number density profiles in ram for Mach numbers of 4 and 8 with analytical approximations for the same values. The approximation is appropriate for a one-dimensional sheath with ramming ions. It is based on the assumption that the electron density drops sharply to zero at the sheath edge and that ions conserve mass inside the sheath. The solution of Poisson's equation is then

$$[\sqrt{(1+\psi)} + 2][\sqrt{(1+\psi)} - 1]^{1/2} = (3\sqrt{8}/4)(\xi_s - \xi) \quad (4)$$

where

$$\psi = -2e\Phi/(mV^2) = M_\lambda^2 \quad (5)$$

$$\xi = (\rho/M)x/a \quad (6)$$

and  $\xi_s$  is the location of the sheath edge, while the equation for the number density is

$$n/n_0 = 1/(1+\psi) \quad (7)$$

where  $n_0$  is the ambient ion number density. In Figure 5, the data points are the values computed by MACH while the curves are computed from Eq. (4). The agreement of the values is everywhere within a few percent of the peak potential.

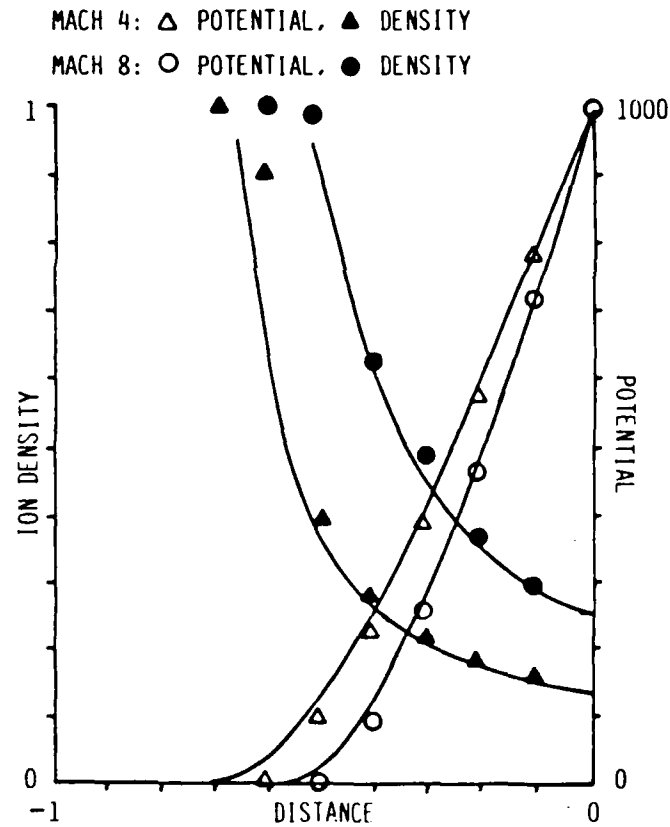


Figure 5. Comparison of MACH Potential and Ion Number Densities in Ram for Mach 4 and 8 With One Dimensional Sheath Contours

It should be emphasized that there are no free parameters in the analytic solutions: for the given plasma conditions, the solutions are determined completely by the potential on the object and by the requirements that the potential and electric field both vanish at the sheath edge.

Figure 6 shows the comparison of MACH potential and number density profiles along the rim direction for Mach 8 with an analytical approximation. The rim direction is here defined to extend from the disk along a line perpendicular to the ram-wake direction. The approximation is not very good and is given for purposes of qualitative comparison only. In this approximation, the potential is computed assuming that it is cylindrically symmetric around the edge of the disk and that the ion number flux into the symmetric sheath is determined by the ion thermal speed and not its bulk speed. The curves are the solutions of Poisson's equation

$$(1/\xi)d(\xi d\chi/d\xi)/d\xi = 2\xi_0/[\xi\sqrt{1+\chi}] \quad (8)$$

$$n/n_0 = \xi_0/[\xi\sqrt{1+\chi}] \quad (9)$$

$$\xi = r/\lambda_D \quad (10)$$

along with a phenomenological modification ( $r \rightarrow \sqrt{r^2 + d^2}$ , where  $d = 0.2a$  is the thickness of the disk) designed to represent the potential as it approaches a disk of finite thickness. It is seen that the potentials are in reasonably good agreement, within a few percent of the peak potential. Again, it is to be emphasized that, aside from the construction of the model (which is only a crude representation, at best), there are no free parameters.

Figure 7 shows the comparison of MACH potential and ion number density profiles on the wake axis for the same Mach numbers with an analytic solution given by Alpert et al:<sup>4</sup>

$$n = n_0 \exp(-M^2 a^2 / z^2) \quad (11)$$

where  $z$  is the distance from the disk. The agreement between computation and the geometric shadowing model shown as solid lines is reasonably good in the far wake region, beyond perhaps three to six disk radii. The overshoot at eight disk radii for Mach 4 and twelve disk radii for Mach 8 is likely of numerical origin; if so, it should be possible to cure it by changing the mesh size. It should be noted that this type of agreement is not expected to hold generally, but is a result of the fact that the case presented can be adequately represented by a quasineutral far wake. If we had assumed that the electrons were dense and energetic, with perhaps the

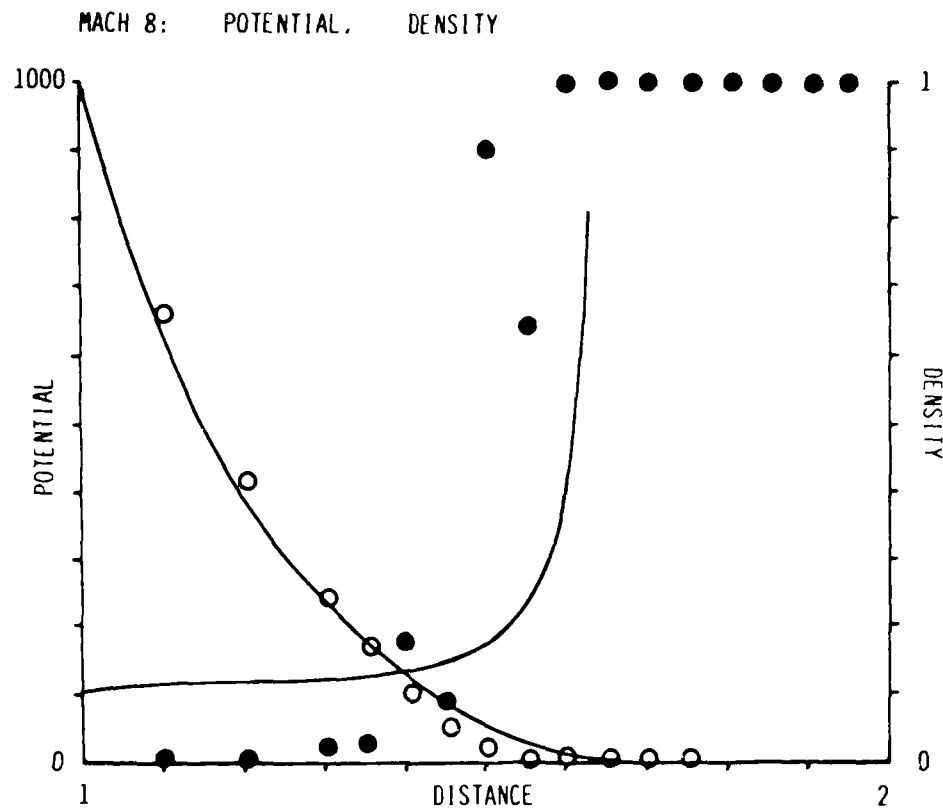


Figure 6. Comparison of MACH Potential and Ion Number Densities Along the Rim Direction With Cylindrical Sheath Contours

10 keV energies characteristic of the auroral environment, we would expect that the structure of the far wake would be largely controlled by ambipolar diffusion; the wake should be substantially shorter because of the transverse acceleration of ions by the diffusion process.

The dashed lines in Figure 7 show the effects of increasing the effective shadowing radius by 25 percent for Mach 4 and 10 percent for Mach 8. The physical basis is that at least part of the sheath must be responsible for geometric shadowing. These increases constitute about one-half and one-quarter of the rim sheath radius, respectively. While increasing the shadowing radii to the full sheath radii gives very bad fits, the smaller increases can reasonably account for the far wake density within a few percent of ambient beyond about three disc radii, with the exceptions of the overshoot regions. This good agreement suggests that the effect of the sheath

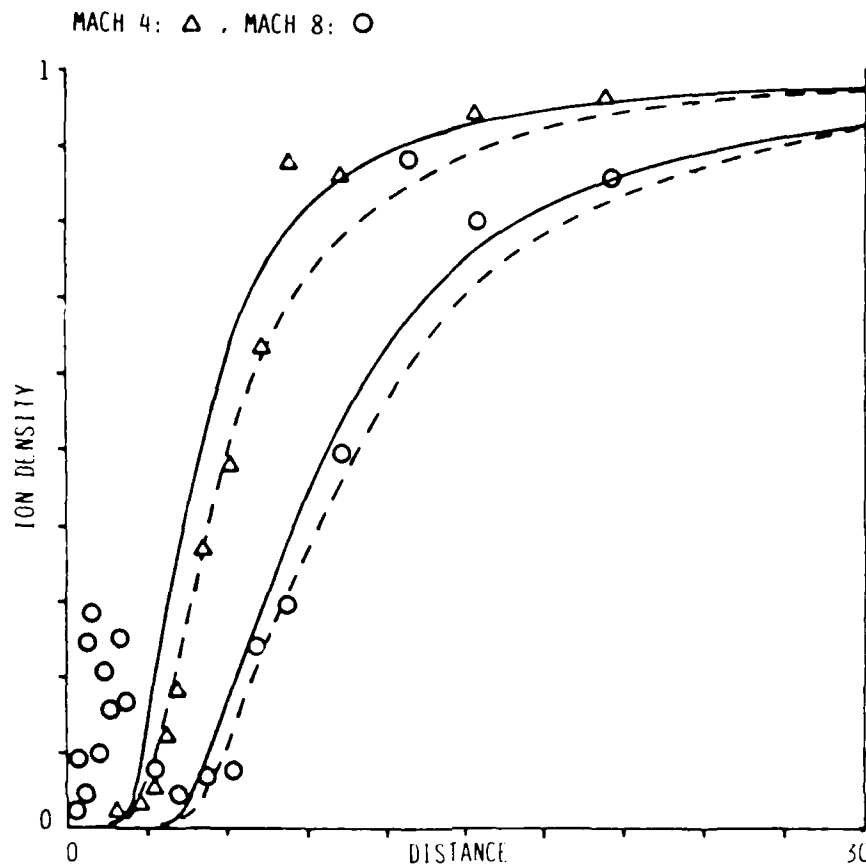


Figure 7. Comparison of MACH Ion Number Density Along Wake Axis With Quasineutral Wake Model Representing Geometric Shadowing for Mach 4 and 8. The solid lines represent geometric shadowing by the disc. The dashed lines represent geometric shadowing by the disk radius plus 25 percent (Mach 4) and 10 percent (Mach 8).

on geometric shadowing in the far wake is Mach number dependent, with smaller effects at higher Mach numbers. While this shadowing effect must be studied in more extensively, these results are satisfactorily fit by the empirical formula:

$$\text{Effective shadowing radius} = a + \text{constant} \cdot t_s / M \quad (12)$$

where  $t_s$  is the sheath thickness. The constant is presumably a function of the vehicle potential; in the case mentioned, the value of the constant is approximately one-half.

The discussion so far has centered on the analytic comparisons which it is possible to make. The MACH computer model is in good agreement with the analytic tests with the exception of the ion density in rim. Aside from the rim density, the outstanding feature which does not fit an analytical model is the existence of the peak in the ion number density inside about three disk radii in wake for Mach 8. While we have not established that it is a genuine feature, we believe this peak is likely to be real based on the discussion associated with Figures 2 and 3. The peak follows the general qualitative trend outlined earlier, including its appearance close to the disk and at high Mach numbers.

#### 4. COMPARISON OF MACH AND POLAR

To test the POLAR code against MACH, we have run POLAR for the same conditions mentioned above. In this section we compare POLAR results with those of MACH. The brief discussion, which covers some of the material discussed above, is intended to address the relative accuracy of both models. Estimates of accuracy are in no way absolute but represent a judgment based on comparison of the models with each other and with analytic approximations. It should be noted that all of these comparisons are at Mach 5 rather than at Mach 4 and 8.

Figures 8a and 8b show POLAR and MACH profiles of electrostatic potential and ion number density, respectively, in ram for Mach 5 along with the solutions of Eq. (4). The POLAR potential is too broad and demonstrates a known tendency of POLAR to increase the sheath thickness by about one grid spacing. As mentioned earlier, this problem can presumably be controlled by running at higher resolution; the operational problem is to balance increased accuracy against increased computation time. The POLAR densities are essentially exact in comparison with Eq. (4); the MACH densities are somewhat too high, a feature not seen in the Mach 4 and 8 results. These errors suggest that the errors in POLAR and MACH are currently on the order of 10 percent of peak values in ram at the spatial resolution shown.

Figures 9a and 9b show the same profiles in the rim direction. The same tendency toward overexpansion of the sheath is apparent. The density profiles show fluctuations on the order of 10 to 20 percent of ambient which may be taken to be the order of magnitude of the error in the models at low resolution.

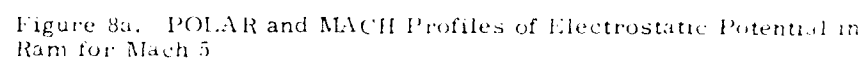
Figure 10 shows ion number density contours in wake. Geometric shadowing by the disk for Mach 5 is shown as a dashed line. MACH shows the geometric shadowing by the disk mentioned above. The difference between MACH and geometric shadowing appears to be unphysical; the MACH data correspond to geometric shadowing by a disk smaller than the actual disk size. POLAR shows similar shadowing; the displacement could reasonably be interpreted as shadowing due to



disk plus sheath except for the fact that only pure disk shadowing exists in POLAR. As such we attribute errors on the order of 10 percent to 20 percent to both MACH and POLAR beyond a few disk radii in wake. Both codes show large density peaks in wake, MACH to twice ambient and POLAR to about 0.7 times ambient. Both figures are surprisingly high. The MACH density peak appears to be unrealistically high. While we have argued that density peaks in wake are likely to be real, these large enhancements leave open the possibility that errors in the near wake are on the order of 100 percent. Only further comparison and possible modification of both codes will establish the truth.

## 5. DISCUSSION

We have compared the results of the MACH and POLAR computer codes for conditions typical of moderate to high voltage negative charging for satellites in low Earth orbit. We find that the models appear to be in general quantitative and qualitative agreement with the features of the interaction which are susceptible to check. The major exception is the tendency of the POLAR wake to represent shadowing by the disk rather than the sheath. We reiterate that the analytic checks in ram and rim have no free parameters aside from the structure of the models. The agreement between the codes and the analytical models in these regions range from reasonably to remarkably good. While the agreement in the far wake has one free parameter (the effective geometric shielding radius), the nature of the shadowing is in reasonable agreement with the physics of the interaction. In addition, we have argued that the occurrence of ion density peaks near the disk in wake is physically reasonable, at least for high enough potential and Mach number. Based on this analysis, we believe that the MACH and POLAR computer codes adequately compute the spacecraft interaction and wake structure. Further work is required to resolve the disagreement between POLAR and MACH on the peak ion density near the disk in the wake.



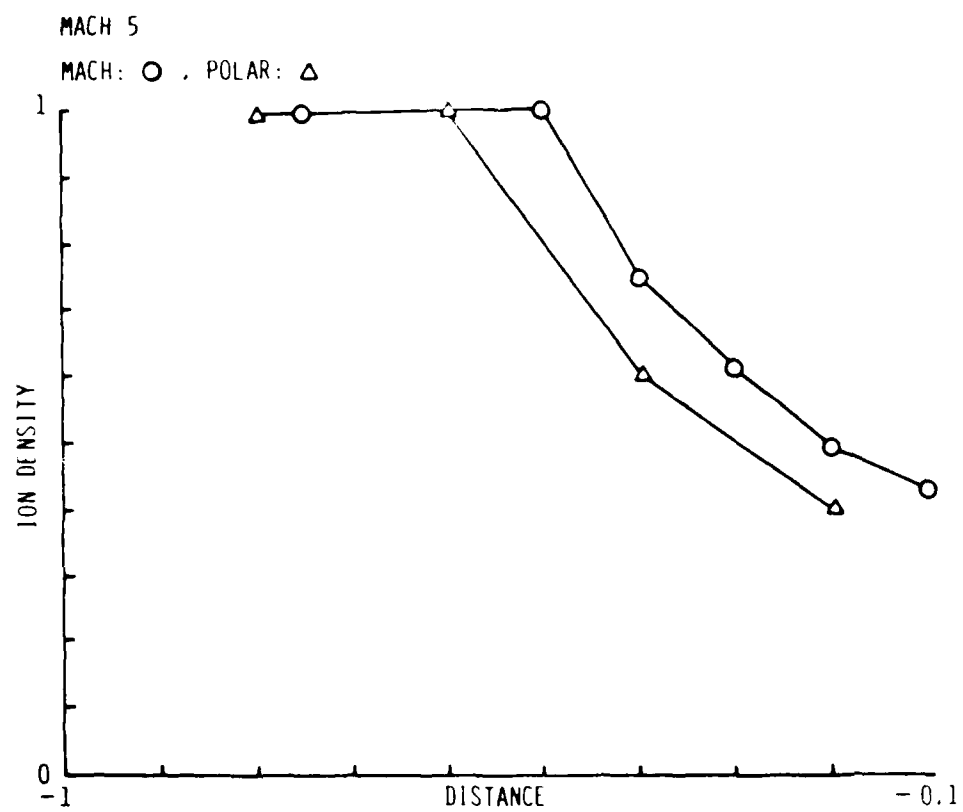


Figure 8b. POLAR and MACH Profiles of Ion Number Density in Ram for Mach 5

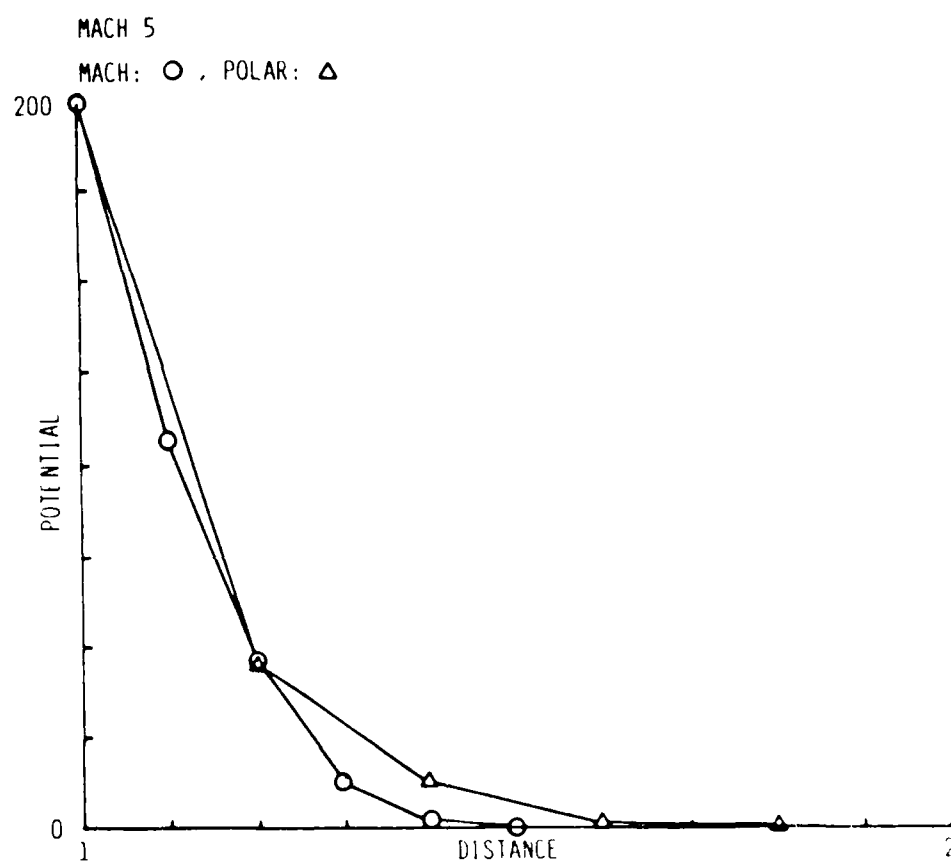


Figure 9a. POLAR and MACH Profiles of File Apostoli - Potential in the Rim Direction for Mach 5

## References

1. Parker, L. W. (1976) NASA Contractor Report No. CR-144159.
2. Parker, L. W., and Sullivan, E. C. (1974) NASA Report No. TN-D-7409.
3. Cooke, D. L., Katz, I., Mandell, M. J., Lilley, J. R., Jr., and Rubin, A. G. (1985) A Three-Dimensional Calculation of Shuttle Charging in Polar Orbit, Spacecraft Environmental Interactions Technology-1983, NASA CP-2359, AFGL-TR-85-0018, p. 229.
4. Alpert, Ya. L., Gurevich, A. V., and Pitaevskii, L. P. (1965) Space Physics With Artificial Satellites, Consultants Bureau, New York.
5. Gurevich, A. V., and Meshcherkin, A. P. (1981) Ion acceleration in an expanding plasma, Sov. Phys. JETP, 53(No. 5):937.

END

3-87

DTIC